# Empirical Validation of Building Energy Modeling for Multi-zones Commercial Buildings in Cooling Season

Piljae Im,[1] Jaewan Joe,[1] Yeonjin Bae,[1] Joshua R. New[1]

[1]Building Technologies Research and Integration Center (BTRIC), Oak Ridge National Laboratory, Oak Ridge, TN, United States

## Abstract

Recent nationwide efforts have provided reliable empirical data for ASHRAE standard 140, "Standard Method of Test for the Evaluation of Building Energy Analysis Computer Programs," to enable improved accuracy of building energy modeling (BEM) engines and improved characterization of their accuracy. Use of reliable empirical validation datasets in the evaluation of BEM tools will lead to more consistent and validated simulation engines across all software vendors. This will expedite the use of BEM in designing new buildings and retrofitting existing buildings, which delivers more energy-efficient buildings.

In this study, a set of validation tests was performed in an occupancy-emulated small office building during a cooling season based on the test plan carefully designed per ASHRAE standard 140. Without making any calibration effort, major building simulation modules such as main heating, ventilation, and air conditioning (HVAC) system and infiltration model are validated with actual experimental data. Finally, an EnergyPlus simulation model was built based on as-built drawings, HVAC specifications, and measured data. Hourly simulation outputs were compared with the measured datasets from the tests to examine the goodness of fit. The generated experimental datasets and model input documentation of the test building will help industries and researchers to validate new BEM tools and improve their simulation engines. The validated simulation models can be leveraged as a rigorously validated benchmark commercial building.

Keyword: Empirical validation, ASHRAE standard 140, EnergyPlus, Infiltration model, Building Energy Model, Rooftop units

# 1 Introduction

## 1.1 Background

Buildings accounts for 40% of all energy use and 75% of total electricity use in United States [1]. Significant efforts have been made to reduce energy in the building sector to conserve natural resources and ensure a sustainable future. Building energy modeling (BEM) has been used to incorporate energy-efficient technologies and designs into new buildings [2] and building retrofits [3, 4] that could result in substantial energy and cost savings. Furthermore, BEM has been used extensively in demonstrating building energy code compliance, supporting green certification, qualification for tax credits and utility incentives, real-time building control [5], building performance analysis [6], and fault detection study [7]. In addition, generic simulation models such as US Department of Energy (DOE) reference building or case 600 in ASHRAE standard 140 [10] are used for investigating predictive control strategies [5], determining cost optimization for thermal energy storage systems [8], and predicting the energy consumption of surrogate building models leveraging machine learning approaches [9]. The legitimacy of these studies completely depends on the credibility of the BEM. However, insufficient characterization of BEM engine accuracy and the resultant lack of confidence have been reported as a limitation of current BEMs and are regarded as a barrier to ensuring the reliability of BEMs. Thus, there is an immediate need for comprehensive validation of BEM tool accuracy.

Recent nationwide efforts are expanding the capability of ASHRAE standard 140. Its objective is to provide a complete empirical validation data set for tool evaluation, as seen in Figure 1, and development beyond the existing classes I and II that utilize the simulation platform. The ASHRAE Standing Standard Project Committee (SSPC) 140 aims to revise and maintain ASHRAE standard 140 by specifying the test methods most effective for evaluating the BEM, specifically, the thermal performance of buildings and HVAC systems. And, as active participants to the SSPC 140, Oak Ridge National Laboratory (ORNL), National Renewable Energy Laboratory (NREL), Lawrence Berkeley National Laboratory (LBNL), and Argonne National Laboratory (ANL) have performed the 3-year (i.e., 2016–2019) multi-laboratory empirical validation project sponsored by the DOE Building Technologies Office (BTO). Major outputs of this project include (1) empirical validation of a multizone with rooftop units (RTUs) system using a flexible research platform (FRP) located at ORNL, (2) empirical validation of an indoor/outdoor modular apartment at NREL, (3) empirical validation of building envelope models with FLEXLAB at LBNL, and (4) uncertainty characterization for experimental measurement at ANL. The project has generated multiyear validation test plans, model input specifications, and more than 20 documented tests and operational configurations.

This study focused on the empirical validation of a multizone office building served by a RTU that is a typical heating, ventilation, and air conditioning (HVAC) system for small to medium offices. A full-scale two-story building with more than 500 sensors for the weather, envelope, thermal zones, and HVAC system in high granularity was tested with simulated occupancy by programmed heaters and humidifiers. The EnergyPlus

simulation model was used as a simulation test bed, considering the complexity of the multizones, pervasiveness of the simulation tools, and the project motivation to facilitate the development of building energy simulation tools. To reduce uncertainties from the different modules in the building energy simulation program, performance-related data for HVAC (i.e., RTU and fan) and infiltration were processed and modeled based on the experiments and then input to the simulation model.

## 1.2 Literature Review

Different approaches for validating the accuracy of BEM under study exist: (1) comparative (e.g., inter-model comparison), (2) analytic and (3) empirical validation methods as defined in ASHRAE standard 140 [10~12]. The comparative study is free from the actual measurements and tests that inevitably require engineering labor and cost. And it is meaningful for analyzing the differences among BEM tools and could lead to improving the internal code. The International Energy Agency (IEA) Building Energy Simulation Test (BESTEST) tested a single-zone model focusing on different building features such as thermal mass, internal heat gain, fenestration, and setpoint [13] followed by multizone diagnostic cases [14]. The analytic method solves the simple heat transfer problem to find the unique solution and compare the results with BEMs that are solved numerically within their internal codes. This approach allows us to understand the BEM code and possibly find existing issues in the code. However, for both approaches, due to the lack of ground truth of the building models, the reliability of the model and its parameters are questionable. In addition, the latter approach is limited to simple cases that can be solved exactly without numerical attempt. On the other hand, the empirical validation method compares simulation results to measured data from a real building or test cell; therefore, this validation methodology has the highest potential to validate building energy simulation tools for accurately predicting actual energy performance. Due to the nature of this methodology, however, significant engineering and instrument cost would be needed to monitor the data to reduce uncertainties in building input parameters. This method would prevail due to the technology development for sensing and data acquisition systems and its deployment to actual buildings.

International efforts directed at developing the empirical validation method have been undertaken by IEA for several decades. Different simulation models were tested against experimental data by international participants focusing on solar impacts on buildings in general and low-energy buildings specifically [15]. Multiple BEMs including TRNSYS and DOE-2 were tested for steady and dynamic cases, both with constant and variable airflow rates. Through the participants' modeling reports, the empirical validation process is carried out systematically; modelers revise their model legitimately after the initial validation exercise with appropriate assumptions as well as modeling specifications. This empirical validation effort proved the validity of the validation process, which involves the modelers and multiple BEMs, and confirmed that most BEM software agrees with actual measurements. However, most experiments were carried out with test cells or a climate chamber with confined environments, which might not reflect real buildings' thermal behaviors or their complexity. One of the most recent empirical validation projects was conducted in IEA's Annex 58 [16]. In this project, as a first phase of the test, the different sets of experimental methods (e.g., co-heating test, free-

floating test, dynamic heating sequences) were carried out using the identical single test cell with various locations and weather conditions using different analysis approaches including the autoregressive with exogenous terms (ARX) model and state–space models to characterize the thermal performance of the cell. Then, the BEM validation exercise was carried out with more than 20 modeling teams to investigate the reliability of the detailed dynamics of BEM, utilizing the full-scale unoccupied residential building with affluent instruments for the measurements. Different building energy simulation programs (e.g., EnergyPlus, TRNSYS, ESP-r) and program languages (e.g., Matlab, Modelica) were tested against two experimental sets by participating modelers [17]. Mostly good agreement among the simulations using multiple BEMs and measurement approaches were shown, except for the blind-involved case. This suggests that the error from user input to the BEM due to the software interface, lack of clarity of the input definition, and lack of user training should be reviewed. Nevertheless, those efforts are limited to investigating the building envelope (i.e., fabric) without considering the HVAC system, which has been suggested as future work for this project. Combining the in-situ experimental data from the HVAC system in empirical validation is required to address the nature of the heat transfer mechanism that is constantly coupled within the building envelope and HVAC system. This is challenging due to their heterogeneous thermal behaviors.

Other validation studies have been carried out based on the actual measurement in a test cell with various building energy simulation programs, including TRNSYS [18, 19], EnergyPlus [20, 21], and multiple BEMs [22], or with a grey-box model as a state–space formulation that consists of resistance and capacitance between the temperature states [19, 23]. The TRNSYS building model is calibrated by increasing the details of the model by including key factors one by one, such as the infiltration, shading, and internal heat gain, until the room air temperature prediction reaches satisfactory accuracy [18]. Inter-model comparisons (i.e., comparative validation) are conducted between the grey-box model and TRNSYS against the actual measurement in a multizone test cell [19], and between EnergyPlus and HELIOUS for the solar gain model against the test cell with different blind configurations [20]; both show good agreement between the simulations and experiments. Multiple programs such as EnergyPlus, TRNSYS, Modelica, and ANSYS Fluent for CFD (Computational Fluid Dynamics) are also investigated in a test cell where the radiant floor system is applied, yielding reasonably good results [22]. However, in many cases, test cells are too simple to reflect the realistic building and its thermal behavior [20, 22, 23]. In addition, validation results of the EnergyPlus simulation compared to the device-level home energy consumption are not good enough even for the annual usage due to the inaccurate building audit (e.g., incorrect appliance/lighting specifications) [21], which emphasizes the significance of the input document for the simulation model.

## 1.3   Objectives

The main objective of the study is to provide the input document (i.e., drawing, thermal properties of the building fabric and fenestration, HVAC performance curve, weather data) and building performance data sets (i.e., energy consumption and temperature profiles) that can be used to validate key functionality in different energy simulation tools and to identify errors and inadequate assumptions in simulation engines so that

developers can correct them. This study, as research work, aims to prove the methodology of the project by validating the EnergyPlus simulation model against two experiments in cooling season based on the input model validation including the infiltration and HVAC models. Extensive experiments including the tracer gas and blower door tests for the infiltration modeling as well as the HVAC system modeling are the unique contribution of this study that significantly contributes the evaluation of the energy usage in building. Also, while previous studies were generally limited to simple cases [11, 16] or multi-zones residential building [17], empirical validation utilizing the FRP would provide unique data sets for more realistic multizone commercial buildings that can be potentially leveraged to revise the current BEM engines and develop the new tools by individual parties or international collaboration. To achieve this final goal, the following tasks were carried out:

- Generated HVAC performance curves for RTU and fan with in-situ experimental data
- Developed an infiltration model with a tracer gas test
- Reviewed the validation test methods in ASHRAE standard 140
- Conducted the validation test for cooling season
- Developed the simulation models with input documentation, developed HVAC performance curves, and developed infiltration model
- Ran the simulation models with weather data and compare with experimental data

The test bed is explained in Section 2 followed by the methodology in Section 3. Sub-system modules are developed in Section 4 and demonstrated in empirical validation in Section 5. Conclusions and future work are discussed in Section 6 and 7, respectively.

## 2    Test Bed

### 2.1    Building characteristics

The two-story FRP, consisting of slabs and a steel superstructure with a footprint of 13.4 m × 13.4 m, is representative of light commercial buildings common to the nation's existing building stock (Figure 2 and Table 1). The FRP has 10 conditioned zones and 2 unconditioned zones (e.g., staircase) with a 0.4 m thick exterior wall. The FRP is an unoccupied research apparatus in which occupancy is emulated by process control of lighting, humidifiers for human-based latent loading, and a heater for miscellaneous electrical loads (MELs). The occupancy emulation would drastically reduce the occupancy behavior related to uncertainty in modeling.

The test building is exposed to natural weather conditions for research and development leading to system- and building-level advanced energy efficiency solutions for new and retrofit applications. To reduce the uncertainty of in-ground heat transfer through the slab, 0.3 m Geofoam EPS46 [$R_{US} - 55$ ($R_{SI} - 9.7$)] insulation was installed in the floor. Windows are evenly distributed, except on the east and north side of the first floor, with a 28% windows-to wall-ratio.

## 2.2 HVAC systems

The multizone HVAC system used for the validation tests incorporate a 44 kW (12.5 ton) RTU and a natural gas furnace. The RTU has a 9.6 energy efficiency rating (EER) with two scroll compressors and one central fan with variable frequency drive (VFD). Each room is conditioned with a variable-air-volume (VAV) box with electric resistance reheat. The original intake for the fresh air in the RTU was blocked to reduce uncertainty in the test results.

## 2.3 Instrumentation and monitoring

The Johnson Controls Metasys system, a dedicated energy management control system, was deployed in the FRP; and the room setpoint temperature, schedule, and other controls were predefined through the Metasys system. The main sensors deployed in HVAC and thermal zones are illustrated in Figure 3. In addition, the data acquisition hardware—including 1 master cabinet, 4 peripheral cabinets, 256 thermistor channels, 256 single-ended voltage channels, 100 thermocouple channels, and 64 frequency input (or 5 V) control channels—is currently deployed in the FRP. The sensors used for monitoring are calibrated.

Measurements include the zone setpoint temperature and humidity; supply and return-air temperature and flow rates; and energy consumption of individual components including a compressor, condenser, supply fan, VAV reheating. The data are available in 1 min, 15 min, and 60 min intervals. A dedicated weather station on the roof of the FRP monitored the weather data including outdoor air temperature; humidity; solar radiation (i.e., direct normal, diffuse, and global); and wind speed and direction.

## 3 Methodology

### 3.1 Input model validation approach

In this study, no exploits of the calibration were made for the simulation model. However, significant factors affecting the model behavior were dealt with in the in-situ experimental data; for example, performance curves were generated from the measurement of actual test bed and input to the simulation model as is. This section discusses the key simulation inputs and explains the experimental settings. The main factors that are input models based on the experimental data are:

- Infiltration
- RTU performance curve
- Fan performance curve

### 3.2 Simulation approach

In this study, the building envelope model and HVAC systems are built and configured in SketchUp [24] and OpenStudio [25], and then input to the EnergyPlus 8.9 [26]. Additional details of the HVAC system are addressed in EnergyPlus.

## 3.3 Evaluation metrics and validation output

In this study, normalized mean bias error (NMBE) and coefficient of variation of the root mean square error [cv(RMSE)] were used for quantifying the deviation between the measurement and simulation (equation 1 and 2). $M$, $S$, and $k$ represent the measurement, simulation, and the number of data, respectively. The upper bar refers to the average of the measurement data. Both show the discrepancy in percentage, so the lower value indicates the more accurate simulation results. Overfitting or underfitting can be detected from the NMBE with a sign.

$$\text{NMBE} = \frac{1}{\bar{M}} \cdot \frac{\sum_{i=1}^{n}(M_i - S_i)}{k} \times 100 \qquad (\text{eq. 1})$$

$$\text{cv(RMSE)} = \frac{1}{\bar{M}} \sqrt{\frac{\sum_{i=1}^{n}(M_i - S_i)^2}{k}} \times 100 \qquad (\text{eq. 2})$$

## 3.4 Measuring points

The measuring points below were used in this validation study. Data will be provided in 60 min resolution.

- Cooling DX electricity consumption (kWh)
- Delivered cooling energy consumption (kWh)
- Supply fan electricity consumption (kWh)
- Total airflow rate (m$^3$/s)
- VAV airflow rate (m$^3$/s)
- Zone air temperature (°C)

Delivered cooling energy consumption was calculated with enthalpy difference between the mixed and supply air based on the ASHRAE fundamental [27] to account for the latent load in RTU.

## 3.5 Experimental setup

ASHRAE standard 140 [10] provides mechanical cooling/heating base cases CE100 and CH100. However, the building/system specifications for these cases are not consistent with the current FRP setup. The FRP is a two-story building with 10 thermal zones exposed to real weather conditions. These cases are not intended to be used with a real building—only with building energy models. The test conditions for cases CE100 and CH100, including the building envelope requirements, are not suitable for any real building. For example, the wall, roof, and floor insulation R-values defined in these cases are less than 100 m$^2$·K/W (567 h·ft$^2$·°F/Btu), and the infiltration rate is zero, which cannot be realized in real buildings. Therefore, the test plan for the multizone HVAC validation refers only to a selected set of ASHRAE standard 140's HVAC test conditions that can be realized in the current FRP setup. Given the objective of this study to provide a set of empirical data from a high-fidelity test facility, this would fulfill the objectives.

ASHRAE standard 140 cases CE100, CE 110, CE 120, CE130, CE 150, CE160, and CE165 were reviewed, and they were applied as described or modified, as applicable to the FRP. An RTU with a VAV was used to perform a cooling season test in summer 2018.

### 3.5.1    Cooling test 1: baseline case

A building "as-is" was tested as a baseline case test. There were no other treatments, such as blocking windows or adding additional envelope insulation. The test included the following additional test conditions:

- Window blinds were not used.

- No sensible or latent internal loads were emulated.

- A fixed discharge temperature of 12.7°C (55°F) for RTU and no Outdoor air (OA) or exhaust air provision (same as CE100) were set.

- Fixed static pressure [i.e., 249Pa (1in.H2O)] was maintained.

- Room thermostat cooling setpoint temperature was maintained at 22.2°C (72°F) with a possible minimum dead band. There was no setback/setup schedule and no humidity control. Heating was turned off including main gas furnace and VAV reheating.

### 3.5.2    Cooling test 2: increased thermostat setpoint

The original test plan included increasing the thermostat setpoint to 26.7°C (80°F) while keeping the other conditions the same as in the cooling baseline case (i.e., test 1). However, based on observations from test 1, the conditions for cooling season test 2 were redefined. The test plan remains the same, but the RTU discharge air temperature was increased to 15.6°C (60°F). The main purpose of test 2 was to reduce the cooling loads by reducing the thermostat setpoint. But, as noticed in test 1, the rooms were overcooled in general, mainly due to the independent controls of the RTU air handling unit (AHU) and VAV boxes, and reducing the thermostat setpoint cannot reduce the cooling load. As the RTU discharge temperature was increased to 15.6°C (60°F), however, the cooling load was reduced as intended for the test 2.

## 4    Subsystem modules development

In this section, we develop the subsystem modules including infiltration model, RTU curve, and fan curve based on the experimental data, which play a major role in building energy simulation programs [e.g., infiltration model impacts on the energy consumption of 3~8% [28]. The subsystem modules are intended to reduce the errors in each module to relieve the uncertainty of the modeling associated with the entire building/HVAC system. In addition, adopting the generic HVAC models from the building simulation programs or the performance data in the product catalog does not guarantee good matches with actual measurement. At best, one can find similar models matching the nominal capacity from the programs, and the performance data in a brochure may differ in actual measurement due to the environmental gap between the test chamber and the site-specific field. Therefore, validating the sub models (i.e., modules in the building simulation program) with actual measurements is required.

### 4.1    Infiltration model updates

A whole building energy model is composed of various component models including a glazing model, HVAC system component, infiltration model, and ground coupling model. Of this, the building infiltration model has

been one of major sources of uncertainty in modeling, mainly due to difficulties in measurement and correlating the infiltration with natural conditions. While infiltration contributes to heating and cooling energy use directly, a number of infiltration models exist, and their impacts on energy consumption vary [29]. Therefore, generalizing the global infiltration model for different buildings is challenging and nearly impossible. A pure simulation study or comparative simulation study may adopt a generic infiltration model in existing building simulation programs. However, a validation study requires experiments such as tracer gas or blower door tests for developing a new model or revising an existing one.

To develop the infiltration model, a tracer gas test is carried out to measure the ACH, and the blower door test is performed to investigate the airflow rate per external wall area (i.e., $I_{design}$ in equation. 4). Then the coefficients representing the environmental impact from the temperature difference between indoor and outdoor and wind speed are estimated with measured ACH and $I_{design}$.

The tracer gas test was performed with a multichannel doser and sampler (INNOVA Air Tech Instrument, 1303 multipoint sampler, and doser) and the photoacoustic gas monitor (INNOVA Air Tech Instrument, 1412 photoacoustic field gas monitor) along with the tracer gas (R134a/tetrafluoroethane) which is a nonflammable refrigerant (Figure 4). Multiple tubes were installed in thermal zones and connected to the doser and sampler. Six thermal zones (room 102, 103, 104, 105, 204, and 206) were selected due to the limitation of the instrument, which can measure only six points simultaneously.

Five sets of the tracer gas test were carried out from the March to June 2019:

- Set 1: 3/14, 14:40~3/15, 1:40
- Set 2: 3/15, 15:10~3/15, 22:00
- Set 3: 3/29, 17:40~3/29, 21:50
- Set 4: 6/4, 11:50~6/4, 19:10
- Set 5: 6/10, 17:10~6/10, 23:10

The gas was injected to the return duct of the AHU for 5~6 min until the gas concentration reached 600 mg/m$^3$ and was distributed to all thermal zones with HVAC operation. The gas concentration (mg/m³) was measured every 5 min. The optional regression method (equation. 3) from the ASTM standard [30] was used to estimate the ACH:

$$ln(C_{i+t}) = -ACH \cdot t + ln(C_i), \qquad \text{(eq. 3)}$$

where

*ACH:* the air change rate (1/h)

$C_i$, $C_{i+t}$: concentration in time *i* and *i+t*, and

*t*: sample time (h).

The blower door test was carried out to identify the airflow rate per external wall area ($I_{design}$) by measuring the airflow rate per building pressure [31]. The HVAC system was off, and all interzone doors were open. The blower door fan was installed at the northern external door on the first floor (Figure 2), and the building was

depressurized. Airflow rate ($m^3$/s) with different pressures from 30 to 70 Pa with 10 Pa increments was measured. Based on the airflow rate per pressure, the $I_{design}$ is calculated with the following equation [29]:

$$I_{design} = (\alpha_{bldg} + 1) \cdot I_{75P} \left( \frac{0.5 C_s \rho U_H^2}{75} \right)^n \qquad \text{(eq. 4)}$$

$I_{75P}$ represents the building leakage ($m^3$/s) at 75 Pa, which is extrapolated from the blower door test. The wind speed at building height ($U_H$), the density of air ($\rho$), the average surface pressure coefficients ($C_s$), urban terrain environment coefficients ($\alpha_{bldg}$), and the flow exponent ($n$) are set to 4.47 m/s, 1.18 kg/$m^3$, 0.1617, 0.22, and 0.65. Taking account for HVAC operation, $I_{design}$ is often reduced by 25% based on suggestions in the literature [29]; this procedure is left for debate as the literature also reports that the comparison of the default EnergyPlus model and the developed model shows different deviation between the HVAC on and off settings [28]. However, we considered more conservative curtailment, a half, which gives 0.00013 $m^3$/(s·$m^2$) (0.0255 CFM/$ft^2$). This value does not deviate from the Building Performance Institute (BPI) standard [32] that yields 0.00011 $m^3$/(s·$m^2$) (0.0210 CFM/$ft^2$) by dividing the $I_{50P}$ by the N factor [33], considering the region and building height.

Infiltration models in EnergyPlus that were addressed in this study included Infiltration Design Flow Rate; these models are based on an old study [34] but can address the environmental impact by the regression. They can still be developed [35, 36] as shown below:

$$Infiltration_{model} = I_{design}(C_0 + C_1|dT| + C_2 V + C_3 V^2) \qquad \text{(eq. 5)}$$

Regression is performed to identify the coefficients ($C_0{\sim}C_3$) using the constrained linear least square function (*lsqlin*) in Matlab. Figure 5 shows the ACH comparison of default models (i.e., two predecessors of EnergyPlus, BLAST, and DOE-2) and measurement and regression results for the five experimental sets. Two defaults are either higher or lower than the measurement, while the regression is close to the measurement. The cv(RMSE) of the default models (i.e., BLAST and DOE-2) are 180.5% and 66.0%, while that of the regressed model is 16.9%.

Table 2 shows the coefficient comparison. The regressed model tended to be less sensitive to the temperature difference and more sensitive to the wind velocity compared to the BLAST model (i.e., $C_1$ is smaller when the $C_3$ is introduced). Estimated coefficients are input to the EnergyPlus object, ZoneInfiltration:DesignFlowRate.

## 4.2  RTU performance curve

The submodel most significantly affecting building energy performance is the HVAC system, which in this study was a packaged DX cooling system. In the EnergyPlus model, the electricity consumption of the DX cooling ($P_{DXcooling}$) is calculated based on three performance curve fits (equation. 6 [26]). Those are polynomial curves (*f*) that are used to characterize the performance of the HVAC equipment, which are the capacity, EIR (Energy Input Ratio), and run-time fraction (RTF) taking account for the cycling impact on energy use. The feature data of those polynomials are two temperatures ($T_{out}$: condenser side outdoor air temperature; $T_{coil}$: wet-bulb air temperature passing the cooling coil), airflow ratio ($m_{ratio}$: ratio of actual and maximum airflow rate), and part load ratio (PLR).

$$P_{DXcooling} = \underbrace{\underbrace{Q_{nominal} \cdot f_{cap}}_{Cooling\ capacity} \cdot \underbrace{\frac{1}{COP_{nominal}} \cdot f_{EIR}}_{Energy\ input\ ratio} \cdot f_{RTF} \cdot h}_{Power\ at\ full\ load} \qquad \text{(eq. 6)}$$

where

$$f_{cap} = \left(c_{cap1} + c_{cap2}T_{out} + c_{cap3}T_{out}^2 + c_{cap4}T_{coil} + c_{cap5}T_{coil}^2 + c_{cap6}T_{out}T_{coil}\right)\left(c_{cap7} + c_{cap8}m_{ratio} + c_{cap9}m_{ratio}^2\right)$$

$$f_{EIR} = \left(c_{EIR1} + c_{EIR2}T_{out} + c_{EIR3}T_{out}^2 + c_{EIR4}T_{coil} + c_{EIR5}T_{coil}^2 + c_{EIR6}T_{out}T_{coil}\right)\left(c_{EIR7} + c_{EIR8}m_{ratio} + c_{EIR9}m_{ratio}^2\right)$$

$$f_{RTF} = \frac{PLR}{\left(c_{PLR1} + c_{PLR2}PLR\right)}$$

To create the performance curve, quasi–steady-state data were filtered from 1 year of HVAC operation data in 1 min resolution; then the transition periods (4 and 6 min data) were excluded for the start and end times. The pivot table was then built to provide the average value of cooling capacity ($Q_{nominal} \cdot fcap$ in equation. 6) and power consumption ($P_{DXcooling}$ in equation. 6) in a full-load condition for different environmental and operational conditions of $T_{out}$, $T_{coil}$, and $m_{ratio}$.

Data with a nominal airflow rate were extracted from the pivot table to estimate the coefficients for temperature modifiers ($C_{cap1} \sim C_{cap6}$) based on the measured cooling capacity. The entire pivot table was then used to identify the airflow modifiers ($C_{cap7} \sim C_{cap9}$). Finally, the rest of the coefficients ($C_{EIR1} \sim C_{EIR6}$ and $C_{EIR7} \sim C_{EIR9}$) were regressed with full-load power consumption in a similar fashion. Constrained linear regression (*lsqlin*) was used in the Matlab environment.

Figure 6 shows the comparison of experimental data and prediction from the regression model. The delivered cooling energy prediction matches well for stages 1 and 2; RMSEs were 0.7 kWh and 1.7 kWh, and correlation coefficients were 0.91 and 0.98. Power consumption prediction also matched well for stages 1 and 2; RMSEs were 0.9kWh and 1.6kWh, and correlation coefficients were 0.97 and 0.98.

Results above are based on the dataset without the on/off loss of the RTU. To investigate the PLR effect and estimate the polynomial of $f_{RTF}$, unfiltered data were applied. One minute data were summed for an hour to capture the hourly power loss due to the on/off operation. The calibrated coefficients are 0.8 and 0.2, which does not deviate significantly from the typical value of 0.85 and 0.15. Figure 7 shows a comparison of power consumption. RMSE, cv(RMSE), and correlation coefficient are 0.45k Wh, 12.1%, and 0.90. The estimated model is input to the EnergyPlus object CoilPerformance:DX:Cooling along with developed curves in Curve:Quadratic and CurveBiquadratic.

## 4.3 Fan performance curve

The fan model was also estimated as shown in Figure 87. The second-order polynomial of the airflow fraction (i.e., actual flow/design flow) and fan power consumption were generated with experimental data from January to June 2019. Only steady-state data were used by excluding the start and end times, and 1 min data were averaged for an hour. Including the potential outliers shown in Figure 8, the correlation coefficient is 0.90. The estimated coefficient is input to the EnergyPlus object Fan:VariableVolume.

## 4.4    Miscellaneous efforts

### 4.4.1    Fenestration

Four windows are evenly distributed on the top floor of the FRP. Distribution of the windows on the ground floor is identical, but the two windows on the north and east side were replaced by glass doors. The windows and a sill cross section are modeled with WINDOW 7.5 [37] and THERM 7.5 [38]. The windows used are thermally broken aluminum frame windows with two panes of 6 mm glass and a 16 mm air gap. The frame width is 61.3 mm with a frame U value of 24.221 $W/m^2K$. The ratio of frame-edge glass conductance to center-of-glass conductance is 1.4. The width of the window is 1,930 mm, and the height is 1,829 mm.

The north and east walls have one door each. The door on the north wall is a single door, while the door on east wall is double door. The door is a thermally broken aluminum frame with projected frame dimension of 190.9 mm and a frame U value of 11.788 $W/m^2K$. The ratio of frame-edge glass conductance to center-of-glass conductance is 1.31. The height of the door is 2,235 mm, and the width of the single door and double door are 1,016 mm and 1,829 mm, respectively. Both windows and doors use the same glazing configurations. The calculated U factor, solar heat gain coefficient (SHGC), and visual transmittance of the glazing properties are 2.68$W/m^2K$, 0.7, 0.786, respectively.

### 4.4.2    Weather data generation

A dedicated weather station on the FRP's roof monitored weather data, and the data corresponding to the test period was provided for building energy modeling. Table 3 contains the full list of weather data variables. Instant data at each hour were used from 1 min data for dry-bulb temperature, relative humidity, atmospheric pressure, and wind speed/direction. Dewpoint temperature is calculated with respect to dry-bulb temperature, pressure, and relative humidity. Sixty minute data were averaged from 1 min data for horizontal infrared radiation intensity (from the sky), global horizontal radiation, direct normal radiation, and diffuse horizontal radiation from measured data.

## 5    Empirical validation results

### 5.1    Test 1 (6/13/2019~6/18/2019)

During test 1, the VAV reheating was turned off. Under this condition, it was observed that room temperature never reached 22.2°C (72°F), except in west-facing rooms during the late afternoon. The low room temperature resulted from the minimum damper positions for 10 VAV boxes. Although the cooling load of a room was met (i.e., no need for cooling), minimum airflow to the room which maintained, and the rooms overcooled. In typical VAV reheating operations, the discharge air should be reheated so as not to overcool the rooms. However, during this test, all reheating was turned off, which might cause overcooling the rooms.

In general, the building energy model uses a constant RTU supply air temperature setpoint as the input parameter, which would result in some discrepancies with the measured supply air temperature. In the simulation, instead of using constant supply air temperature setpoint, the measured hourly supply air temperature was input to the model to reduce this discrepancy.

*Weather conditions*

Figure 9 shows the hourly outdoor air temperature and solar radiation during the test 1 period. The data show that the first 4 days were sunny with increasing outdoor air temperatures and clear sky. The remaining 2 days were relatively cloudy, whereas the temperature at night was relatively high and daily temperature range was smaller. During the test period, the maximum and minimum outdoor air temperatures were ~31°C (88°F ) and ~9°C (48°F), respectively.

*HVAC operations*

Figure 10 shows the measured and simulated hourly profiles of the RTU supply fan electricity consumption and airflow rate. The predictions show a good match with the measurement; NMBE and cv(RMSE) are −0.4%, 1.1% and −0.1%, 0.7%, respectively.

Figure 11 shows the delivered cooling energy between the RTU's mixed and supply air (i.e., enthalpy difference) and electricity consumption of the cooling DX (i.e., compressor and condenser fan). Mostly, the prediction shows a good match with the measurement, except for the electricity consumption of the DX cooling coil at peak (i.e., on the fourth day), which might be due to the stage transition (i.e., triggering stage 2). In addition, the following day shows the discrepancy on the delivered cooling energy and DX cooling coil consumption. NMBE and cv(RMSE) were -0.2%, 7.8% and −1.9%, 7.5%, respectively.

The total building HVAC electricity consumption (i.e., cooling DX electricity + fan electricity) of the simulation and measurement are compared in Figure 12. It shows that the simulation is about 1.4% lower than the measurement.

*Zone temperature*

In comparisons of room air temperatures, most simulated temperature profiles follow the experimental data. RMSE of each room ranges from 0.39°C to 1.79°C, and NMBE and cv(RMSE) of weighted-average temperature is −2.7% and 4.4% while the maximum deviation is 0.79°C, as shown in Figure 13. Results for the south-facing zone on the second floor (e.g., room 205) appear to be less accurate than other zones exposed to solar radiation.


## 5.2    Test 2 (7/11/2019~7/15/2019)

Based on observations from test 1, the conditions for the cooling season test 2 were redefined. All the original test plan remained the same, but the RTU discharge air temperature increased to 16.7°C (62ºF). With the original 12.8°C (55ºF), basically, test 2 would have the same results as test 1. The main purpose of test 2 was to reduce the cooling loads by reducing the thermostat setpoint. However, as noted in test 1, the rooms are overcooled mainly due to the independent controls of the RTU AHU and VAV boxes, and reducing the thermostat setpoint does not reduce the cooling load. As the RTU discharge temperature was increased, however, the cooling load was reduced as intended.

Figure 14 shows the hourly outdoor air temperature and solar radiation during the test 2 period. The data show that 5 days are similar to test 1 in outdoor air temperature, with a narrow daily temperature range of <10℃. During the test period, the maximum and minimum outdoor air temperatures were ~31℃ (88⁰F) and ~21℃ (70⁰F), respectively.

*HVAC operations*

Figure 15 shows the measured and simulated hourly profiles of the RTU supply fan electricity consumption and airflow rate. The airflow rate of each VAV is not constant; likewise, in test 1, the supply air temperature of the AHU is raised and the VAV dampers modulate more to maintain the room air temperature at the room air temperature setpoint. Simulation does not perfectly follow the measurements, especially when the VAV dampers open beyond the minimum position. This is due to the deviation of the room air temperature that is originated from the limited realization of the heat transfer phenomena at the room level. NMBE and cv(RMSE) are −2.2%, 4.3% and −4.1%, 7.3%, respectively.

Figure 16 shows the delivered cooling energy between the mixed and supply air of the RTU (i.e., enthalpy difference) and electricity consumption of the cooling DX (i.e., compressor and condenser fan). The prediction generally shows a good match with the measurement. However, for the delivered cooling, the simulation does not follow the fluctuation of the measurements at night. This fluctuation results from the enthalpy of the RTU supply air whereas the simulation uses only the measured temperature (see section 5.1), while the RTU return air has the input of the temperature and humidity from the weather file. NMBE and cv(RMSE) for the delivered cooling and cooling DX are −4.0%, 11.5% and −0.7%, 8.9%, respectively.

The total building HVAC electricity consumption (cooling DX electricity + fan electricity) of the simulation and measurement are compared in Figure 17. It shows that the simulation returns results ~1.3% lower than the measurement.

*Zone temperature*

In comparisons of room air temperatures, most simulated temperature profiles follow the experimental data. RMSE of each room ranges from 0.51℃ to 1.35℃, and NMBE and cv(RMSE) of weighted-average temperature are −1.5% and 3.4%, respectively, while the maximum deviation is 1.14℃ (Figure 18). Results for the south-facing zone on the second floor (e.g., room 205) appear to be less accurate than other zones.

# 6 Conclusions

In this study, a systematic approach for empirical validation of the commercial building was carried out to provide reliable building data sets for BEM tool improvement and development focusing on the building envelope as well as the HVAC systems. Building infiltration, RTU DX cooling, and fan models were estimated with in-situ experimental data and then input to the EnergyPlus simulation model. Two sets of cooling season tests were performed, and the results were compared with the EnergyPlus simulation model built from the as-built drawings and developed models without the calibration efforts.

The study's major findings are as follows:

- The existing default infiltration models are not matched well with experiments and had to be revised to show good agreement with the experiments; cv(RMSE) is improved from 180.5% and 66.0% to 16.9%.

- RTU DX cooling and supply fan models were developed with experimental data; the correlation coefficient for both was 0.90.

- Two sets of the validation experiments were carried out for 5~6 days each in cooling season. Delivered cooling energy in RTU, electricity consumption (i.e., RTU DX cooling and fan), and room air temperature were compared and showed a good match between the simulation and experiment. The deviation of the total electricity consumption is 1.3~1.4%, and the maximum deviation of the room air temperature is 0.79~1.14°C.

## 7  Discussion and Future work

During the test, several challenges and limitations in measurement and simulation were identified, suggesting possible future work.

- **Zone mixing:** The current EnergyPlus model does not adequately address interzone mixing unless one uses a detailed airflow network model. Interzone air mixing, which occurs in a real building and impacts indoor temperatures, should be investigated further.

- **Infiltration model:** The infiltration rate behaves differently between the HVAC on and off. The model developed in this study only accounts for the phenomena during HVAC on. A different set of the model parameters can be identified for the HVAC off case with a free-floating test. Also, even though the extensive tracer gas and blower door tests were carried out, the infiltration model developed in this study can be site-specific. The robust infiltration model can be developed with further experiments with different buildings that can be potentially generalized to other buildings.

- **Heating test:** A heating test validation tests were carried out and will be discussed in the near future.

- **Uncertainty quantification:** As a part of multilaboratory efforts, ANL is performing an uncertainty quantification of the measured data and simulation input uncertainties. Given the nature of empirical validation, this work will provide better metrics to compare the measured data with the simulation results. Results of this effort will be published in the near future.

- **Different tools:** This study only focuses on EnergyPlus. Multiple BEMs can be investigated with the existing experimental dataset to improve the reliability of the dataset and possibly compare the capability of the different BEMs.

- **Building energy modeling practice:** Only basic building data along with HVAC data can be distributed, and participating modelers can try validation. The comparative study can be carried out in parallel to validate the project methodology.

# Acknowledgment

# References

[1] US Department of Energy (2011), Buildings Energy Data Book. https://ieer.org/resource/energy-issues/2011-buildings-energy-data-book/.

[2] Feng, K., Lu, W., & Wang, Y. (2019). Assessing environmental performance in early building design stage: An integrated parametric design and machine learning method. *Sustainable Cities and Society*, *50*, 101596. https://doi.org/10.1016/j.scs.2019.101596.

[3] Shen, P., Braham, W., & Yi, Y. (2018). Development of a lightweight building simulation tool using simplified zone thermal coupling for fast parametric study. *Applied energy*, *223*, 188-214. https://doi.org/10.1016/j.apenergy.2018.04.039.

[4] Shen, P., Braham, W., & Yi, Y. (2019). The feasibility and importance of considering climate change impacts in building retrofit analysis. *Applied energy*, *233*, 254-270. https://doi.org/10.1016/j.apenergy.2018.10.041.

[5] Gholamibozanjani, G., Tarragona, J., De Gracia, A., Fernández, C., Cabeza, L. F., & Farid, M. M. (2018). Model predictive control strategy applied to different types of building for space heating. *Applied energy*, *231*, 959-971. https://doi.org/10.1016/j.apenergy.2018.09.181.

[6] Moreci, E., Ciulla, G., & Brano, V. L. (2016). Annual heating energy requirements of office buildings in a European climate. *Sustainable Cities and Society*, *20*, 81-95. https://doi.org/10.1016/j.scs.2015.10.005.

[7] Zhang, R., & Hong, T. (2017). Modeling of HVAC operational faults in building performance simulation. *Applied Energy*, *202*, 178-188. https://doi.org/10.1016/j.apenergy.2017.05.153.

[8] Kamal, R., Moloney, F., Wickramaratne, C., Narasimhan, A., & Goswami, D. Y. (2019). Strategic control and cost optimization of thermal energy storage in buildings using EnergyPlus. *Applied Energy*, *246*, 77-90. https://doi.org/10.1016/j.apenergy.2019.04.017.

[9] Edwards, R. E., New, J., Parker, L. E., Cui, B., & Dong, J. (2017). Constructing large scale surrogate models from big data and artificial intelligence. *Applied Energy*, *202*, 685-699. https://doi.org/10.1016/j.apenergy.2017.05.155.

[10] ASHRAE standard 140-2014 (2014). Standard 140-2014: Standard Method of Test for the Evaluation of Building Energy Analysis Computer Programs. *ASHRAE, Atlanta*.

[11] Judkoff, R., Wortman, D., O'doherty, B., & Burch, J. (2008). *Methodology for validating building energy analysis simulations* (No. NREL/TP-550-42059). National Renewable Energy Lab.(NREL), Golden, CO (United States).

[12] Judkoff, R., & Neymark, J. (2006). *Model validation and testing: The methodological foundation of ASHRAE Standard 140* (No. NREL/CP-550-40360). National Renewable Energy Lab.(NREL), Golden, CO (United States).

[13] Judkoff, R., & Neymark, J. (1995). *International Energy Agency building energy simulation test (BESTEST) and diagnostic method* (No. NREL/TP--472-6231). National Renewable Energy Lab. www.nrel.gov/docs/legosti/old/6231.pdf.

[14] Neymark, J., Judkoff, R., Alexander, D., Felsmann, C., Strachan, P., & Wijsman, A. (2011). *IEA BESTEST multi-zone non-airflow in-depth diagnostic cases* (No. NREL/CP-5500-51589). National Renewable Energy Lab.(NREL), Golden, CO (United States).

[15] Travesi, J., Maxwell, G., Klaassen, C., Holtz, M., Knabe, G., Felsmann, C., Achermann, M., & Behne, M. (2001). Empirical validation of Iowa energy resource station building energy analysis simulation models. *IEA Task*, *22*. http://www.task39.iea-shc.org/data/sites/1/publications/Iowa_Energy_Report.pdf.

[16] Erkoreka, A., Gorse, C., Fletcher, M., & Martin, K. (2016). EBC Annex 58 Reliable Building Energy Performance Characterisation based on full scale dynamic measurements.

[17] Strachan, P., Svehla, K., Heusler, I., & Kersken, M. (2016). Whole model empirical validation on a full-scale building. *Journal of Building Performance Simulation*, *9*(4), 331-350. https://doi.org/10.1080/19401493.2015.1064480.

[18] O'Donovan, A., O'Sullivan, P. D., & Murphy, M. D. (2019). Predicting air temperatures in a naturally ventilated nearly zero energy building: Calibration, validation, analysis and approaches. *Applied Energy*, *250*, 991-1010. https://doi.org/10.1016/j.apenergy.2019.04.082.

[19] Cattarin, G., Pagliano, L., Causone, F., & Kindinis, A. (2018). Empirical and comparative validation of an original model to simulate the thermal behaviour of outdoor test cells. *Energy and Buildings*, *158*, 1711-1723. https://doi.org/10.1016/j.enbuild.2017.11.058.

[20] Loutzenhiser, P. G., Manz, H., Carl, S., Simmler, H., & Maxwell, G. M. (2008). Empirical validations of solar gain models for a glazing unit with exterior and interior blind assemblies. *Energy and Buildings*, *40*(3), 330-340. . https://doi.org/10.1016/j.enbuild.2007.02.034.

[21] Glasgo, B., Hendrickson, C., & Azevedo, I. L. (2017). Assessing the value of information in residential building simulation: Comparing simulated and actual building loads at the circuit level. *Applied Energy*, *203*, 348-363. . https://doi.org/10.1016/j.apenergy.2017.05.164.

[22] Nageler, P., Schweiger, G., Pichler, M., Brandl, D., Mach, T., Heimrath, R., Schranzhofer, H & Hochenauer, C. (2018). Validation of dynamic building energy simulation tools based on a real test-box with thermally activated building systems (TABS). *Energy and buildings*, *168*, 42-55. *Energy and Buildings* 168: 42–55. https://doi.org/10.1016/j.enbuild.2018.03.025.

[23] Del Barrio, E. P., & Guyon, G. (2004). Application of parameters space analysis tools for empirical model validation. *Energy and buildings*, *36*(1), 23-33. https://doi.org/10.1016/S0378-7788(03)00039-2.

[24] Sketchup, https://www.sketchup.com/ (accessed Jan 2019).

[25] OpenStudio, OpenStudio sketch-up extension. (2019). https://extensions.sketchup.com/sv/content/openstudio-100 (accessed Jan 2019).

[26] EnergyPlus. (2019). US Department of Energy. https://energyplus.net/ (accessed January 2019).

[27] ASHRAE. (2013). ASHRAE Handbook, Fundamentals.

[28] Ng, L. C., Quiles, N. O., Dols, W. S., & Emmerich, S. J. (2018). Weather correlations to calculate infiltration rates for US commercial building energy models. *Building and environment*, *127*, 47-57. https://doi.org/10.1016/j.buildenv.2017.10.029.

[29] Gowri, K., Winiarski, D. W., & Jarnagin, R. E. (2009). *Infiltration modeling guidelines for commercial building energy analysis* (No. PNNL-18898). Pacific Northwest National Lab.(PNNL), Richland, WA (United States). https://doi.org/PNNL-18898.

[30] ASTM International. Standard E741-00. (2006). Standard Test Method for Determining Air Change in a Single Zone by Means of a Tracer Gas Dilution. West Conshohocken, PA: ASTM International.

[31] TEC (The Energy Conservatory). (2017). Model 3 Minneapolis Blower Door™. https://energyconservatory.com/wp-content/uploads/2017/08/All-Blower-Door-Guides.pdf.

[32] BPI. (2012, January 4). Technical Standards for the Building Analyst Professional. BPI standard. http://www.bpi.org/sites/default/files/Technical%20Standards%20for%20the%20Building%20Analyst%20Professional.pdf.

[33] Sherman, M. (1995). The Use of Blower-Door Data. *Indoor Air* 5 (3): 215–224. https://doi.org/10.1111/j.1600-0668.1995.t01-1-00008.x.

[34] Coblentz, C. W., & Achenbach, P. R. (1963). Field measurements of air infiltration in ten electrically-heated houses. *Ashrae Transactions*, *69*(1).

[35] Ng, L., Persily, A., & Emmerich, S. (2014a). Infiltration in Energy Modeling: A Simple Equation Made Better. *ASHRAE Journal* 56 (7): 70–72.

[36] Ng, L. C., Emmerich, S. J., & Persily, A. K. (2014b). An Improved Method of Modeling Infiltration in Commercial Building Energy Models. NIST Technical Note 1829. http://dx.doi.org/10.6028/NIST.TN.1829.

[37] LBNL. (2019a). A Computer Program for Calculating Total Window Thermal Performance Indices, WINDOW Version 7.5. https://windows.lbl.gov/software/window (accessed Sep 13, 2019).

[38] LBNL. (2019b). Two-Dimensional Building Heat-Transfer Modeling, THERM Version 7.5. https://windows.lbl.gov/software/therm (accessed Sep 13, 2019).

**Nomenclature**

| Symbol | Description | Units |
|---|---|---|
| ACH | air change rate | 1/hour |
| $ACH_{model}$ | Air Change Rate of infiltration model | 1/hour |
| $C_0 \sim C_3$ | coefficients of infiltration model | - |
| $C_{cap1} \sim C_{cap6}$ | capacity coefficients for temperature modifiers | - |
| $C_{cap7} \sim C_{cap9}$ | capacity coefficients for airflow modifiers | - |
| $C_{EIR1} \sim C_{EIR6}$ | energy input ratio coefficients for temperature modifiers | - |
| $C_{EIR7} \sim C_{EIR9}$ | energy input ratio coefficients for airflow modifiers | - |
| $C_i$ | concentration in time $i$ | mg/m$^3$ |
| $COP_{nominal}$ | nominal coefficient of performance (COP) | - |
| $C_s$ | average surface pressure coefficients | - |
| cv(RMSE) | coefficient of variation of the root mean square error | % |
| $dT$ | temperature difference between zone air and outdoor air | °C |
| $f_{cap}$ | polynomial capacity curve | - |
| $f_{EIR}$ | polynomial energy input ratio curve | - |
| $f_{RTF}$ | function of run-time fraction | - |
| $I_{75P}$ | building leakage at 75 Pa | m$^3$/s |
| $I_{design}$ | airflow rate per external wall area | m$^3$/s·m$^2$ |
| $k$ | number of data | - |
| $M_i$ | measurement data in time $i$ | - |
| $\bar{M}$ | average of the measurement data | - |
| $m_{ratio}$ | ratio of actual and maximum airflow rate | % |
| $N$ | the flow exponent for infiltration model | - |
| NMBE | normalized mean bias error | % |
| $P_{DXcooling}$ | DX electricity consumption | kWh |
| $Q_{nominal}$ | nominal capacity | kW |
| $RMSE$ | root mean square error | - |
| $S_i$ | simulation data in time $i$ | - |
| t | sample time | Hour |
| $T_{coil}$ | wet bulb air temperature passing the cooling coil | °C |
| $T_{out}$ | outdoor air temperature | °C |
| $U_H$ | wind speed at building height | m/s |
| $V$ | wind speed | m/s |

| Greek symbol | Description | Units |
|---|---|---|

| $\alpha_{bldg}$ | urban terrain environment coefficients for infiltration model | - |
| $\rho$ | density of air | kg/m$^3$ |
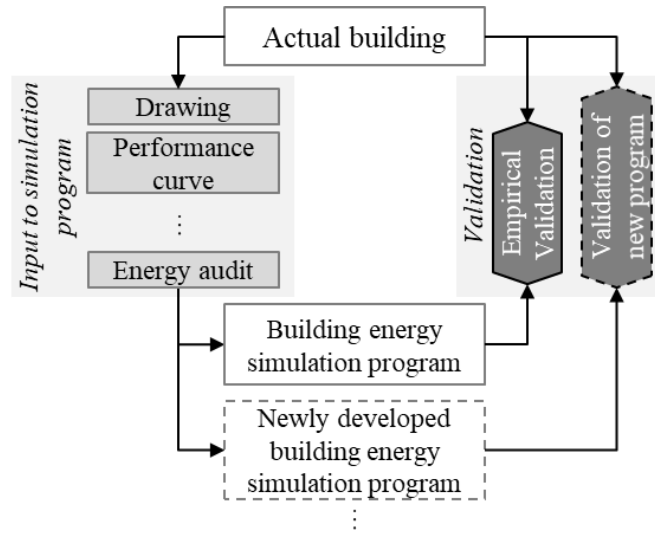


*Figure 1. Conceptual diagram of the project.*

*Figure 2. Front view(top) and plan drawing (bottom).*
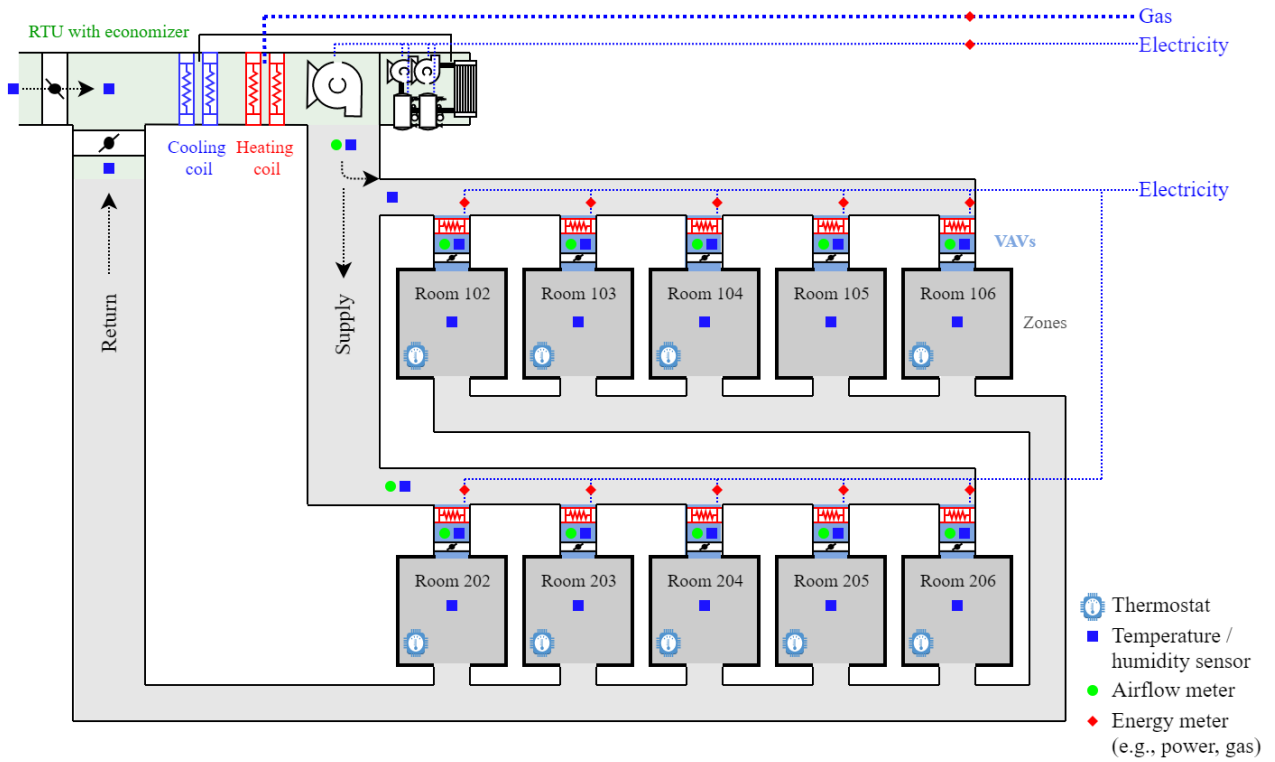


*Figure 3. HVAC and room layout with sensor location*



*Figure 4. Test set: multichannel doser and sampler.*
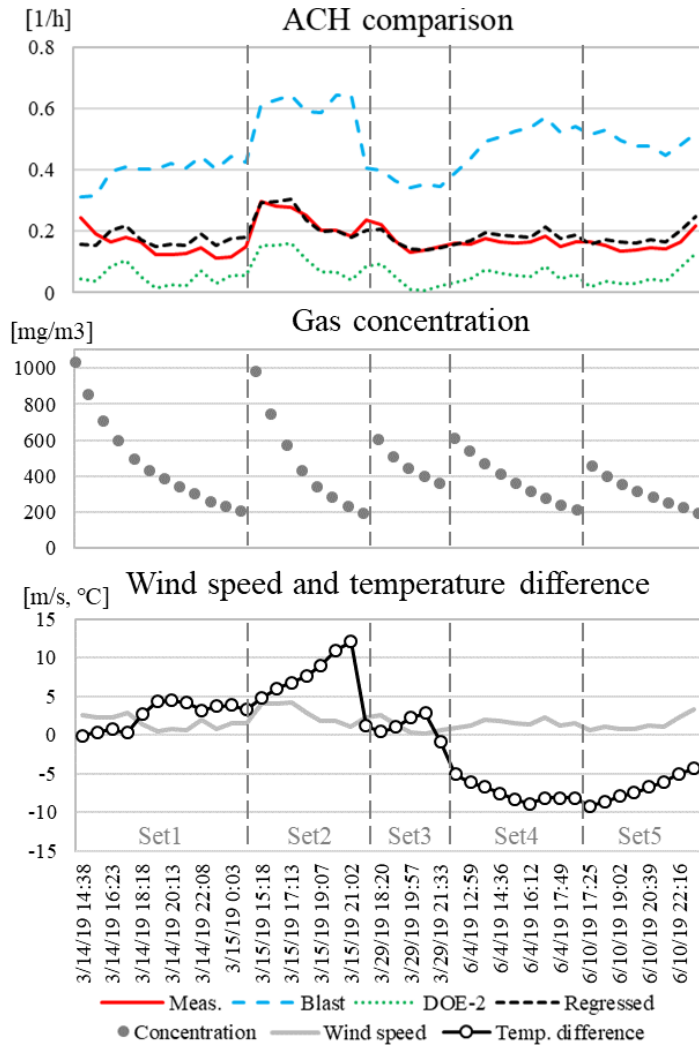
*Figure 5. ACH comparison of measurement and simulations (top) along with a gas concentration (middle) and wind speed and temperature difference (bottom).*
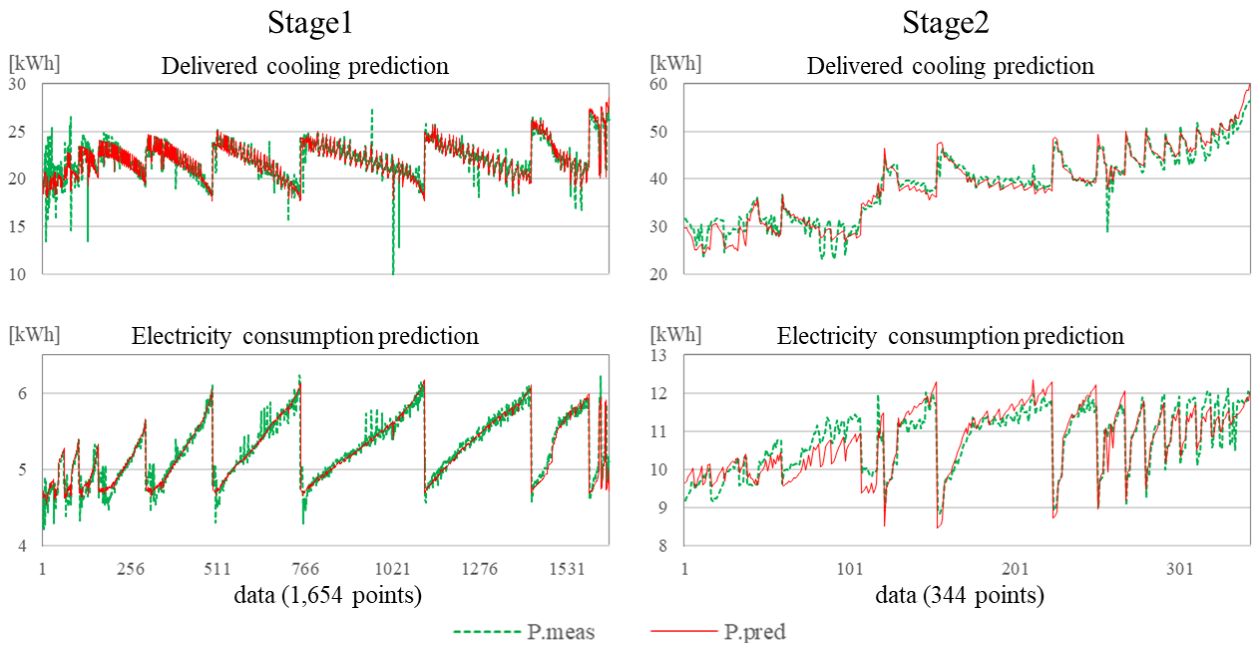
*Figure 6. Cooling capacity (Q) and electricity consumption ($P_{DXcooling}$) prediction for stages 1 (left) and 2 (right).*
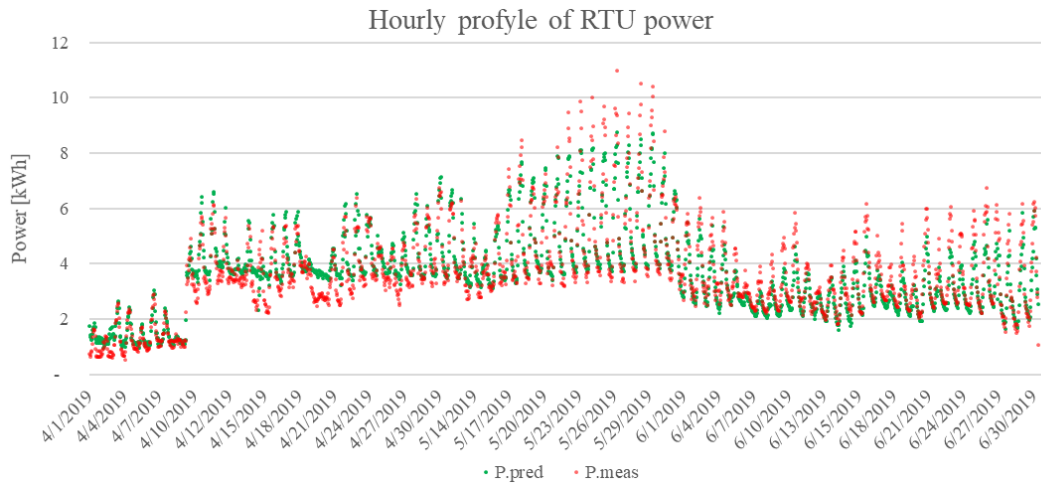


*Figure 7. Power consumption prediction considering PLR loss.*



$$y = -1244.2x^2 + 3432.2x + 10.553$$
$$R^2 = 0.8991$$
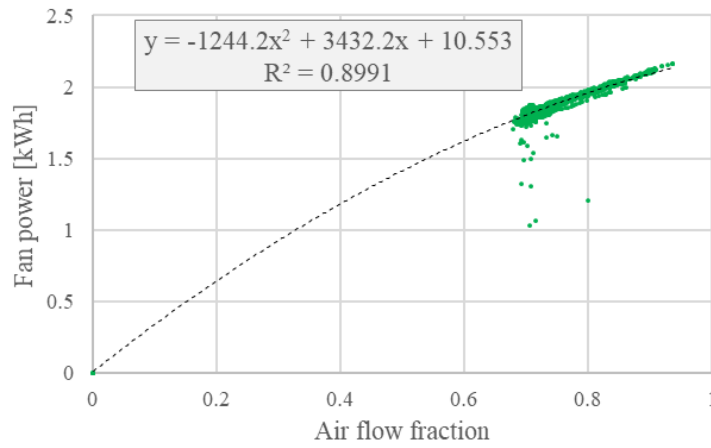
*Figure 8. Fan model validation.*
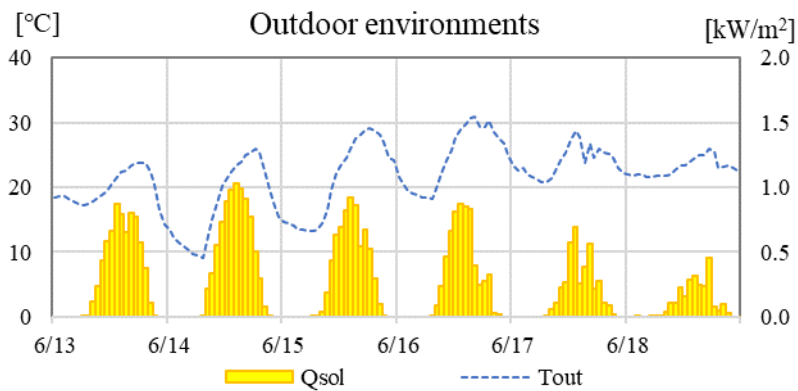


*Figure 9. Hourly outdoor air temperature and solar radiation for test 1.*
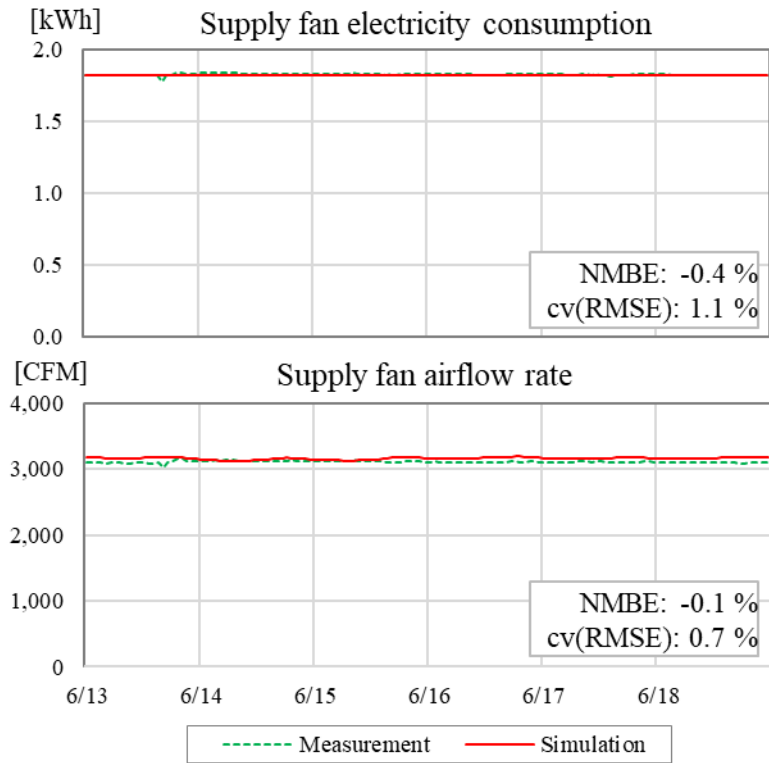
*Figure 10. Hourly RTU fan energy (top) and airflow rate (bottom) for test 1.*
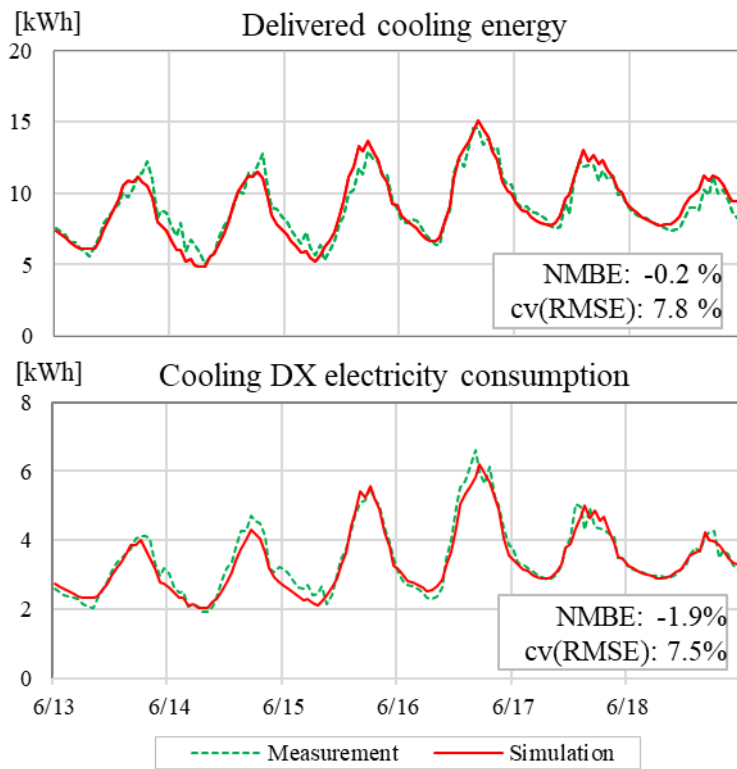


*Figure 11. Hourly delivered cooling energy (top) and electricity consumption (bottom) for test 1.*

## Total RTU Electricity Consumption
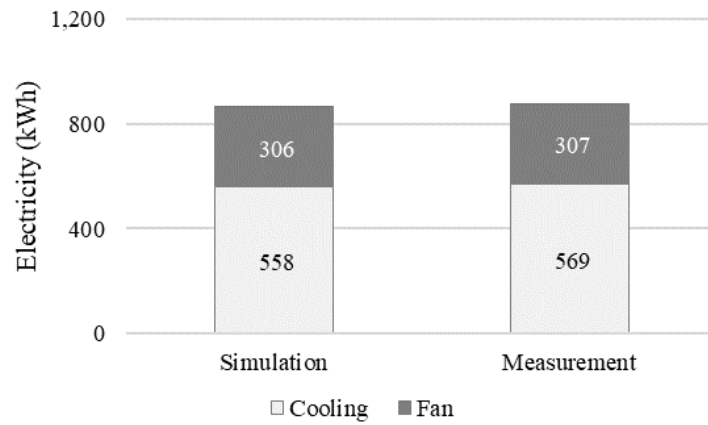


*Figure 12. Total HVAC energy comparison for test 1.*
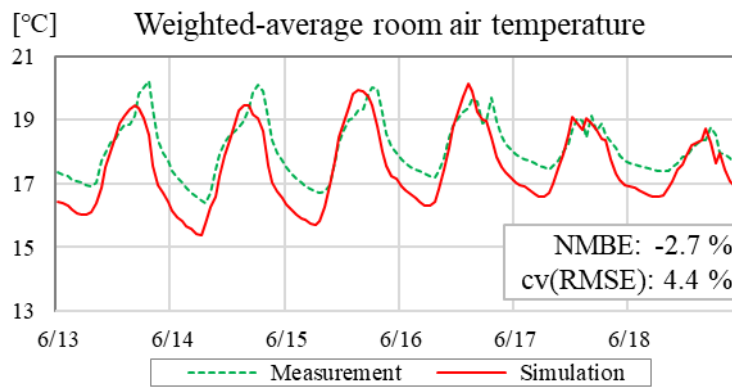


*Figure 13. Weighted-average room air temperature comparison for test 1.*
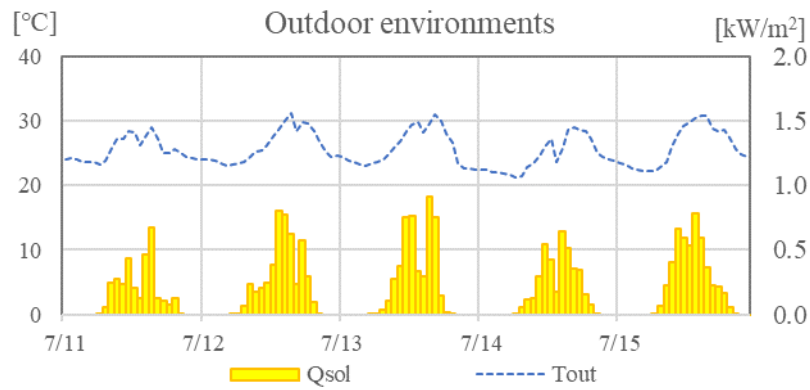


*Figure 14. Hourly outdoor air temperature and solar radiation for test 2.*
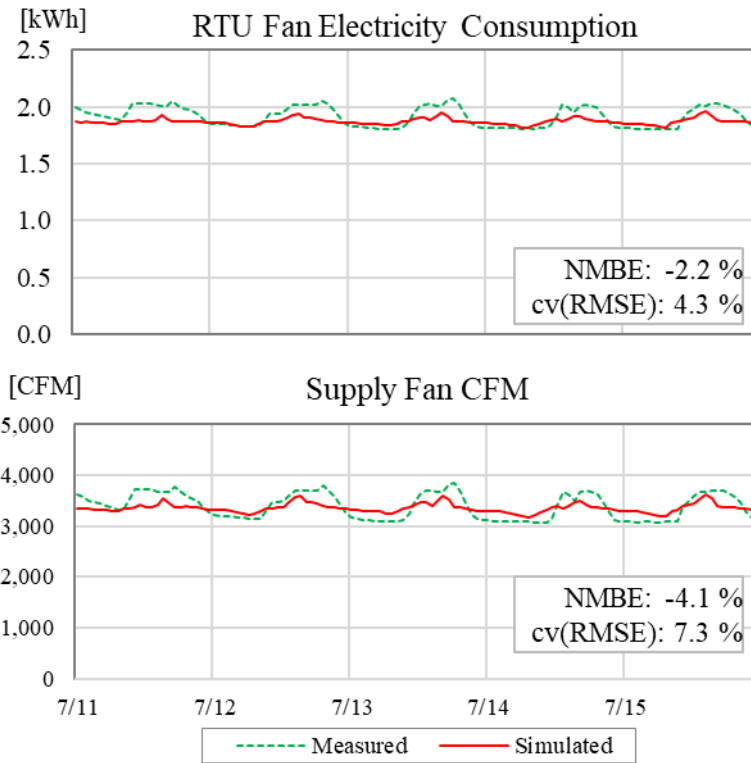
*Figure 15. Hourly RTU fan energy (top) and airflow rate (bottom) for test 2.*
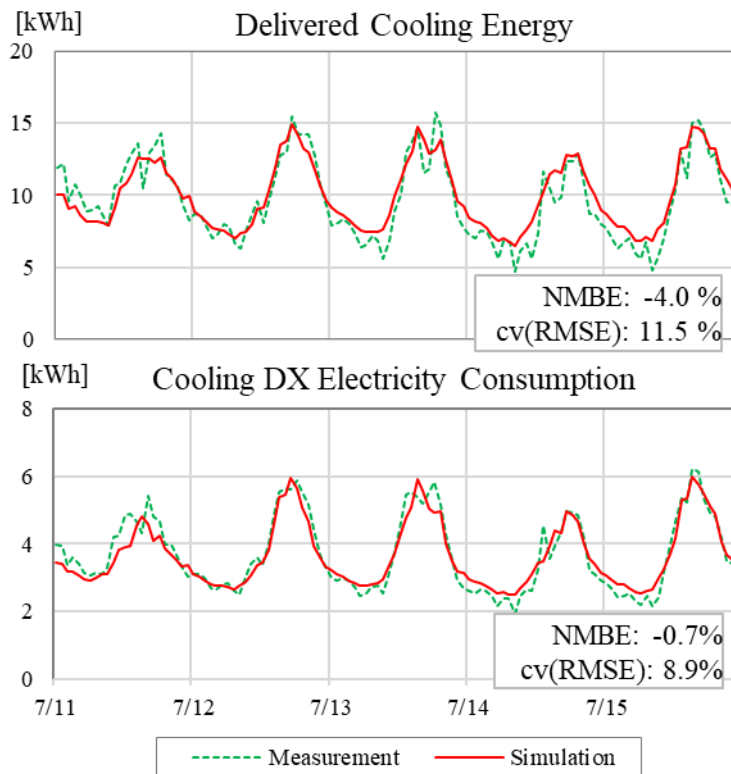


*Figure 16. Hourly delivered cooling energy (top) and electricity consumption (bottom) for test 2.*

## Total RTU Electricity Consumption
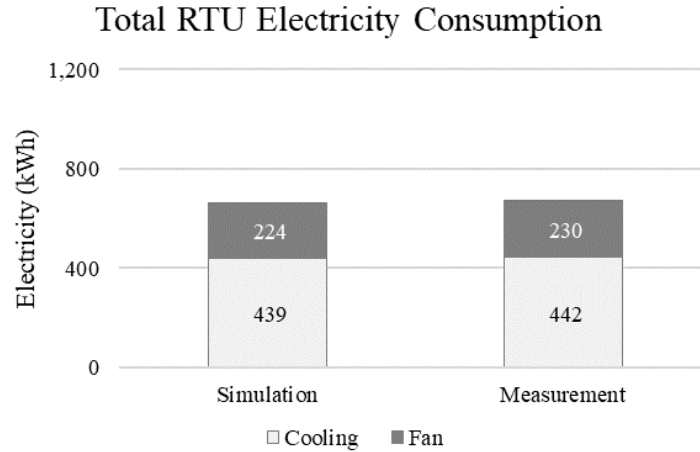


*Figure 17. Total HVAC electricity comparison for test 2.*
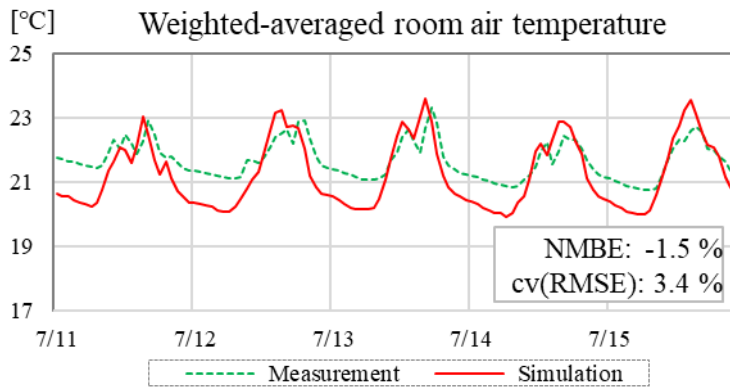


*Figure 18. Weighted-average room air temperature comparison for test 2.*

*Table 1. Descriptions of FRP*

| Location | Oak Ridge, TN, USA |
|---|---|
| Building size | Two-story, 12.2 m×12.2 m (40 ft × 40ft), 4.3 m (14 ft) floor-to-floor height |
| Exterior walls | Concrete masonry units with face brick, $R_{SI}$−1.9 ($R_{US}$−11) fiberglass insulation |
| Floor | Slab-on-grade |
| Roof | Metal deck with $R_{SI}$ −3.17 ($R_{US}$ −18) polyisocyanurate insulation |
| Windows | Double-pane clear glazing, 28% window-to-wall ratio |
| Baseloads | Lighting density: 9.18 W/m$^2$ (0.85 W/ft$^2$), Equipment density: 14.04 W/m$^2$ (1.3 W/ft$^2$) |
| HVAC system | 44 kW (12.5 ton) and 9.7 EER rooftop unit<br>81% annual fuel utilization efficiency (AFUE) natural gas furnace<br>VAV with electric reheat |

*Table 2. Coefficients of default models and regressed model.*

| Models | $C_0$ | $C_1$ | $C_2$ | $C_3$ |
|---|---|---|---|---|
| BLAST | 0.606 | 0.03636 | 0.1177 | 0 |
| DOE-2 | 0 | 0 | 0.224 | 0 |
| Regressed | 0.77004 | 0.00645 | 0.10840 | 0.02483 |

*Table 3. Weather data variables and units.*

| Weather data variables | Units |
|---|---|
| Timestamp | TS |
| Outdoor air temperature | Deg C |

| Outdoor relative humidity | % |
| Barometric pressure | Pa |
| Wind speed | m/s |
| Wind direction | Deg |
| Global radiation | W/m² |
| Direct normal radiation | W/m² |
| Diffuse radiation | W/m² |
| Horizontal infrared radiation intensity from sky | W/m² |